

Geometric depolarization in patterns formed by backscattered light

David Lacoste,¹ Vincent Rossetto,² Franck Jaillon,³ and Herve Saint-Jalmes³¹Laboratoire de Physico-Chimie Theorique, ESPCI,
10 rue Vauquelin, F-75231 Paris Cedex 05, France²Laboratoire de Physique et Modelisation des Milieux Condenses,
Maison des Magistres, B.P. 166, 38042 Grenoble Cedex 9, France³Laboratoire de Resonance Magnetique Nucleaire,
Methodologie et Instrumentation en Biophysique,
UMR CNRS 5012, Domaine de la Doua - CPE - 3,
rue Victor Grignard, 69616 Villeurbanne, France

We formulate a framework for the depolarization of linearly polarized backscattered light based on the concept of geometric phase, i.e Berry's phase. The predictions of this theory are applied to the patterns formed by backscattered light between crossed or parallel polarizers. This theory should be particularly adapted to the situation in which polarized light is scattered many times but predominantly in the forward direction. We apply these ideas to the patterns which we obtained experimentally with backscattered polarized light from a colloidal suspension.

PACS numbers:

The transport of light through human tissues is one of the most promising technique to detect in a noninvasive way for instance breast cancer. Formedical imaging applications, it is important to extract the information contained not only in the intensity but also in the polarization of backscattered light. This is not easy in general due to the complexity of vector-wave multiple scattering. In this paper we study a simple experiment, in which polarized light is backscattered from a diuse medium. In these conditions, one observes between crossed polarizers a fourfold symmetry pattern which was first interpreted qualitatively by Dogariu and Asakura [1]. Recently more quantitative approaches have been developed for Mie scatterers using Mueller matrices [2]. A rather good agreement has been found between the experimental shapes of the patterns and the theoretically predicted ones [2, 3, 4].

In this paper, we propose an alternate approach, which is very simple to implement because it is not based on a vector radiative transfer method as used generally in the literature. Instead our approach is based on the notion of geometric phase, which was introduced by Berry [5] in his interpretation of the experiments showing optical activity in an helically wound optical fiber [6]. So far, the concept has been mostly applied to quantum mechanics and to field theory but has not been used in the context of the transport of polarization in random media except in the recent ref. [7], which we follow and extend in this paper. Before presenting our framework, we discuss the cross-shaped patterns using the Stokes formalism to make contact with previous work [2, 3, 4].

The Stokes parameters are the elements of the vector $I = (I; Q; U; V)$ which is defined with respect to a plane of reference containing the direction of propagation. If the plane of reference is rotated through an angle θ , the new Stokes vector is $L(\theta)I$ where $L(\theta)$ is a rotation matrix

[3]. We used the scattering matrix S corresponding to a distribution of spherical scatterers. The incident light is linearly polarized, is described by a Stokes vector I_0 and is normal to the medium. Since the medium has cylindrical symmetry, the S matrix is independent of θ . After going through an analyzer (with Mueller matrix A), the outgoing Stokes vector is $A \cdot L(\theta) \cdot S \cdot L(\theta) \cdot I_0$. This means that the outgoing intensity in the crossed polarized (resp. copolarized) channel is

$$I_{\perp} = \frac{1}{4} (2S_{11} + S_{33} - S_{22}) - \frac{1}{4} (S_{22} + S_{33}) \cos 4\theta; \quad (1)$$

$$I_{\parallel} = \frac{1}{4} (2S_{11} - S_{33} + S_{22}) - S_{12} \cos 2\theta + \frac{1}{4} (S_{22} + S_{33}) \cos 4\theta; \quad (2)$$

corresponding to Stokes parameters $I = I_{\perp} + I_{\parallel}$ and $Q = I_{\parallel} - I_{\perp}$. Note that according to Eq. 1 the crossed-polarized pattern has a four-fold symmetry, whereas according to Eq. 2, we see that the copolarized pattern contains in addition a two-fold symmetry due to the term proportional to S_{12} [4]. In the particular case, which is satisfied in multiple light scattering [8], when $S = S_{11} \text{diag}(1; C; C; D)$, with $C = S_{22} = S_{33}$ and $D = S_{44} = S_{11}$, Eqs. 1-2 take the simple form

$$I_{\perp} = \frac{1}{2} I_0 (1 - C \cos 4\theta); \quad (3)$$

$$I_{\parallel} = \frac{1}{2} I_0 (1 + C \cos 4\theta); \quad (4)$$

corresponding to outgoing Stokes parameters $I = I_0 = S_{11}$ and $Q = C I_0 \cos 4\theta$. Note that a cross is expected now in both polarization channels and that C measures the contrast of these patterns. We have shown here that the patterns follow from general properties of symmetry

independently of the order of scattering or of the degree of coherence of the source.

Let us now discuss the geometric depolarization of linearly polarized light. For Rayleigh scattering, the (linear) polarization vector after scattering E^0 is $E^0 = k^0 (E \cdot k)$, in terms of the polarization vector before scattering E and the scattered wavevector k^0 . This implies that E evolves by parallel transport in the limit of small scattering angles, and diffuse on the sphere of wavevector directions until the memory of the polarization has been lost. Akkermans et al. has shown that this leads to a depolarization with a characteristic depolarization length ℓ_p equal to $\ell_p = \ln(10)/7 \approx 2.8 \ell$ [9]. Recently ℓ_p was measured using polarization resolved DWS [10], which confirmed Akkermans' prediction for Rayleigh scatterers, and which gave $\ell_p \approx \ell$ in the limit of forward-peaked scattering, in agreement with Monte Carlo simulations [11]. Here we assume forward-peaked scattering because it applies to many biological tissues, and because in this case there is a clear analogy between light scattering paths and semi-flexible polymers [7]. Recently, this analogy has been put on a solid basis, by realizing that the Fokker-Planck (FP) equation which describes semi-flexible polymers can be derived from the radiative transfer equation in this limit [12]. In the following, we carry further the analogy by discussing the degrees of freedom of twist (polymer) analogous to polarization (light scattering).

Let us consider a path of light, which we assume to be normally incident on a semi-infinite random medium. Following ref. [5], we express the polarization vector E in a basis of two vectors $(n; b)$ normal to the tangent vector u (if the path is regular enough, the Frenet frame is a possible choice) as shown in figure 1:

$$E(t) = c_1(t)n(t) + c_2(t)b(t); \quad (5)$$

where t is a parameter which goes from 0 to s along the path. Let us call θ , the angle between E and n at $t = 0$, so that $c_2(0) = c_1(0) = \tan \theta$. Since the polarization evolves by parallel transport $\dot{c}_1 = -\tau c_2$ and $\dot{c}_2 = \tau c_1$, where τ denotes the torsion on the trajectory, as found many years ago by Rytov [13]. In the backscattering geometry, $n(t = s) = n(t = 0)$ and $b(t = s) = b(t = 0)$, therefore we find that the polarization vector at the end of the path is

$$E(t = s) = \cos(\theta + \phi(s))n(s) + \sin(\theta + \phi(s))b(s); \quad (6)$$

where $\phi(s)$ is a geometrical phase, equal to the opposite of the integral of the torsion between $t = 0$ and $t = s$ modulo 4π [5]. In the analogy between a path of light and a semi-flexible polymer, the twist of the path is zero for light (it would be non-zero only in chiral medium), and the writhing angle is precisely ϕ . This writhing is a real value since the path is open, and that value is equal to the algebraic area of a random walk on a unit sphere,

with the constrain that the path goes from the north pole to the south pole in the backscattering geometry. From Eq. 6, we find that the output intensity after the light has gone through an analyzer crossed with respect to the direction of the incident polarization, is proportional to $\sin^2(\theta + \phi)$. Because the medium is random, this intensity must be averaged with respect to all paths:

$$I_2(R) = \int_0^Z P^0(s; R) ds \langle \sin^2(\theta + \phi(s)) \rangle; \quad (7)$$

where $P^0(s; R)$ is the distribution of path length for a given distance to the incident beam R , and $\langle \cdot \rangle$ denotes the average over paths of length s . After expanding the r.h.s of Eq. 7, we obtain the form of Eq. 3 with $I_0(R) = \int_0^Z P^0(s; R) ds$ and the contrast is

$$C(R) = \frac{1}{I_0(R)} \int_0^Z P^0(s; R) ds \langle \cos(2\phi(s)) \rangle; \quad (8)$$

The factor $\cos(2\phi)$ in Eq. 8 means that the contrast results from grouping pairs of paths of opposite geometrical phases, and the sum over s means that the phases of any other paths are uncorrelated. Interestingly a similar dephasing occurs in the theory of magneto-conductance of Anderson insulators [14].

To evaluate the distributions of ϕ for fixed s , $P(s; \cdot)$ shown in fig. 2, we use a Monte Carlo algorithm originally developed for semi-flexible polymers. Random paths are generated with an exponential distribution of path length with a characteristic step equal to the elastic mean free path ℓ . The incident photons are normal to the interface, but when exiting the medium all outgoing angles of emergent photons are accepted. The paths can be generated for an arbitrary ratio of the transport mean free path to the elastic mean free path $\ell^* = \ell$. The geometrical phase are calculated by closing the paths on the momentum sphere with a geodesic [7]. Because of this closure, the distribution of ϕ for short paths $s \ll \ell$ is peaked at zero as is also found for planar random walks (Levy's law). For long paths $s \gg \ell$, the distribution of ϕ widens, until the polarization is completely lost. In this regime, the distribution $P(s; \cdot)$ is gaussian as required by the central limit theorem (the variance which was quadratic for $s \ll \ell$ becomes linear for $s \gg \ell$ as seen in fig. 2), which implies that $\langle \cos(2\phi(s)) \rangle$ is a decreasing exponential function of s . In Fig. 3, we show the corresponding curve for the contrast of the pattern calculated from Eq. 8, together with experimental points, which we obtained by averaging the Stokes parameter Q of an image along two perpendicular directions thereby suppressing a possible contribution in $\cos(2\phi)$ present in Eq. 2. In the experiment, a colloidal suspension of latex particles of negligible absorption (diameter 0.5 μm , wavelength = 670 nm) was used and the sample was about 8.8 μm thick [4]. The value of the anisotropy parameter g in the simulation was chosen to match the experimental value $g = 0.82$. In this

gure, we see that the contrast decreases exponentially as function of the distance R with a characteristic distance of the order of λ_p both in the theory and in the experiments in agreement with refs. [10]–[11]. In the central region of the pattern, low order scattering is dominant as confirmed numerically. This could explain the discrepancy between experiments and simulations in this region, since our model only treats low order scattering events in an approximate way.

To conclude, we have developed in this paper a simple theoretical framework for geometric depolarization, which we have applied to the experimental backscattering patterns. The mechanism of geometric depolarization is general provided that the scattering is peaked in the forward direction. We hope that our work will motivate further theoretical studies on the role of geometric phases in the transport properties of polarization in random media.

We acknowledge many stimulating discussions with T. Maggs, M. C. Bittre, F. Monti, and B. A. van Tiggelen.

Phys. Rev. E, 49, 1767–1770 (1994).

- [12] A. D. Kim and J. B. Keller. "Light propagation in biological tissue," *J. Opt. Soc. Am. A*, 20, 92–98 (2003).
 - [13] S. M. Rytov. "Sur la transition de l'optique ondulatoire l'optique geometrique," *C. R. Acad. Science*, 18, 263–266, (1938).
 - [14] J. P. Bouchaud. "A theory of magnetoconductance in Anderson insulators," *J. Phys. IFrance*, 985–991 (1991).
-
- [1] M. Dogariu and T. Asakura. "Photon pathlength distribution from polarized backscattering in random media," *Opt. Eng.*, 35, 2234–2239 (1996).
 - [2] S. Bartel and A. H. Hiescher. "Monte Carlo simulations of the diffuse backscattering Mueller matrix for highly scattering media," *Applied Optics*, 39, 1580–1588 (2000).
 - [3] M. J. Rakovic, G. W. Kattawar, M. M. Ehnubooglu, B. D. Cameron, L. V. Wang, S. Rastegar, and G. L. Cot. "Light backscattering polarization patterns from turbid media: theory and experiment," *Applied Optics*, 38, 3399–3408 (1999).
 - [4] F. Jaillon. "Caracterisation optique des milieux diffusants: simulation Monte-Carlo et mesures en retrodiffusion polarisee," PhD thesis, University Claude Bernard-Lyon I, Lyon (2003).
 - [5] M. V. Berry. "Interpreting the anholonomy of coiled light," *Nature*, 326, 277–278 (1987).
 - [6] A. Tomita and R. Y. Chiao. "Observation of Berry's topological phase by use of an optical fiber," *Phys. Rev. Lett.*, 57, 937–940 (1986).
 - [7] V. Rossetto and A. C. Maggs. "Writting geometry of sti polymers and scattered light," *Eur. Phys. J. B*, 29, 323–326 (2002).
 - [8] I. Freund and E. Barkai. "Third-order polarization correlations in highly random media," *J. Opt. Soc. Am. A*, 8, 1559–1567 (1991).
 - [9] E. Akkermans, P. E. Wolf, R. Maynard, and G. Maret. "Theoretical study of the coherent backscattering of light by disordered media," *J. Phys. France*, 49, 77–98 (1988).
 - [10] L. F. Rojas, D. Lacoste, P. Schurtenberger, R. Lenke, and F. Scheidl. are preparing a manuscript to be called "Depolarization of backscattered linearly polarized light."
 - [11] D. Bicoût, C. Brosseau, A. S. Martinez, and J. M. Schmitt. "Depolarization of multiply scattered waves by spherical diusers: Influence of the size parameter,"

List of Figures

Fig. 1: Representation of a typical path in a semi-infinite random medium in backscattering. The Frenet frame consists of the tangent \mathbf{u} , the normal \mathbf{n} , and the binormal vectors. R denotes the distance between end points, θ is the initial angle between the polarization vector \mathbf{E} and the normal \mathbf{n} , and Ω is the geometric phase.

Fig. 2: Distribution of the geometric phase for different values of the path length s and in the inset variance of the distribution as function of s/l^* .

Fig. 3: Contrast as function of R : the crosses have been obtained from Monte-Carlo simulations using Eq. 8 and the squares are experimental values, obtained from an analysis of the Stokes parameter Q .



FIG. 1: Representation of a typical path in a semi-infinite random medium in backscattering. The Frenet frame consists of the tangent \mathbf{u} , the normal \mathbf{n} , and the binormal vectors. R denotes the distance between end points, θ is the initial angle between the polarization vector \mathbf{E} and the normal \mathbf{n} , and Ω is the geometric phase.

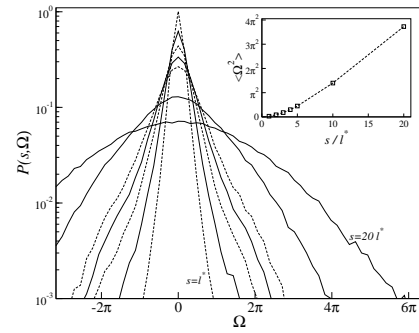


FIG. 2: Distribution of the geometric phase for different values of the path length s and in the inset variance of the distribution as function of s/l^* .

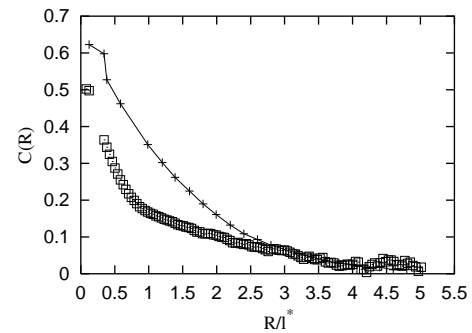


FIG. 3: Contrast as function of R : the crosses have been obtained from Monte-Carlo simulations using Eq. 8 and the squares are experimental values, obtained from an analysis of the Stokes parameter Q .